Environmental Science Nano

ROYAL SOCIETY OF CHEMISTRY

PAPER

View Article Online
View Journal | View Issue

Cite this: *Environ. Sci.: Nano*, 2022, **9**, 1845

Hazard assessment of ingested polystyrene nanoplastics in *Drosophila* larvae†

Mohamed Alaraby,[ab] Doaa Abass,[ab] Josefa Domenech,[a] Alba Hernández[a] and Ricard Marcos *[a]

Micro- and nanoplastics (MNPLs) are intentionally produced for commercial uses (primary MNPLs) or are formed from environmentally aged plastics (secondary MNPLs). Independent of their origin, all of them will finally end up in the environment constituting some of the known emergent pollutants. Despite the inert nature of plastics, questions about their potential biological effects on human health need to find sound answers. In addition, the association between the potentially induced effects and the MNPL size is also required to be known. In this context, we have used our *in vivo* model of *Drosophila* larvae and three nanopolystyrene plastics (PSNPLs) sized 50, 200, and 500 nm (PS-50, PS-200, and PS-500) to add new data to better understand the potential health risks of MNPLs. Our model has permitted us to visualize (*via* transmission electron microscopy, TEM) the journey of the PSNPLs administered *via* ingestion, their interaction with gut lumen components (including symbiotic microbiota), their uptake by gut enterocytes, their translocation through the intestinal barrier to the hemolymph, and their uptake by hemocytes. This behavior was observed for the three analyzed sizes and, for the largest sizes, changes in size/shape were observed in ingested PSNPLs. Although no relevant toxicity, as measured by the egg-to-adult viability, was observed, exposure induced a wide molecular response altering the expression of genes involved in the general stress response, in the antioxidant response and even in the genotoxicity response, as well as in genes related to the intestinal damage response. Furthermore, a general induction of ROS production and DNA damage was also detected. Interestingly, these types of responses were size-dependent with the small PSNPL size inducing a higher response.

Received 27th December 2021,
Accepted 1st March 2022

DOI: 10.1039/d1en01199e

rsc.li/es-nano

Environmental significance

Micro/nanoplastics (MNPLs) are wide-spread environmental pollutants requiring new data to know more about the probable health risks associated with their exposure. Since the main exposure route is ingestion, we have tried to answer different unsolved questions using three different sizes of polystyrene nanoplastics (PSNPLs) in an *in vivo* model of *Drosophila*. As a novelty, we have extensively characterized their interaction with the intestinal barrier of the *Drosophila* larvae by using TEM, detailing, step by step, the journey of PSNPLs ending in the enterocyte uptake and posterior translocation. The biologically evaluated effects were oxidative stress, gene expression changes, and genotoxicity. It is important to emphasize that no similar studies on this topic have been found in the literature.

Background

Plastic wastes are polluting every point of our planet. This is extremely alarming in oceans where millions of tons of plastic wastes accumulate, mainly in the subtropical gyres.[1] Unfortunately, and despite the actions that are being carried out, these pollution levels are expected to continue to grow in the following years.[2] Although special emphasis is focused on the environmental effects of gross plastic wastes, the effects of micro- and nano-products resulting from plastic degradation are gaining interest, mainly as potential factors affecting human health.[3] Micro and nanoplastics (MNPLs) resulting from the degradation of plastic items, known as secondary MNPLs, are considered a new group of emergent contaminants requiring intensive efforts to evaluate their potential effects on health. It must be stated that there are MNPLs tailored at the micro/nano size to be used for different purposes, which are denoted as

[a] *Group of Mutagenesis, Department of Genetics and Microbiology, Faculty of Biosciences, Universitat Autònoma de Barcelona, Campus of Bellaterra, 08193 Cerdanyola del Vallès, Barcelona, Spain. E-mail: ricard.marcos@uab.es; Fax: +34 93 581 23 87; Tel: +34 93 581 20 52*
[b] *Zoology Department, Faculty of Sciences, Sohag University, 82524, Sohag, Egypt*
† Electronic supplementary information (ESI) available. See DOI: 10.1039/d1en01199e

primary MNPLs. One example of this type of MNPL is nano/microbeads extendedly used in the production of cosmetics. Although there are no reliable data on the production of such MNPLs, the results of a survey indicated that in Europe their annual production is about 6.8×10^5 metric tons, although this amount could vary for a factor of 10.[4] Nevertheless, and independent of their origin as primary or secondary MNPLs, they will all finally end up as plastic debris into the environment. Although the environmental concentrations of MNPLs are disputable, mainly for NPLs, the concentration of MPLs could reach 3.35×10^6 particles per m^3 in sediments and 5.57 particles per m^3 in water, as determined in the German Elbe river.[5]

Although the number of studies aiming to produce sound data to be used for the risk assessment of MNPL exposure is exponentially growing, there are still many gaps mainly related to the identification of their mechanisms of action. In this way, it is difficult to obtain shreds of evidence that environmental MNPL pollutants can cause human exposure and health effects.[6,7] Alternatively, *in vivo* approaches can constitute appropriate ways to find sound data linking MNPL exposure and biological effects on the evaluated organisms. Nevertheless, although the reported results using mouse models suggest that accumulation of MNPLs in mammals would likely have negative effects, their long-term consequences are unclear.[8] Due to the complexity and the cost of using mammalian models, together with many posed ethical issues, the use of more simple *in vivo* models is gaining interest. Among these alternative *in vivo* models *Drosophila* stands out.[9]

Drosophila is a pioneering *in vivo* model widely used to determine the harmful effects of a wide set of agents, including different categories of micro and nano-sized materials.[9,10] A new field termed Drosophotoxicology was proposed to highlight the many advantages of this new-old model to evaluate the health effects of environmental pollutants.[11] Since about 75% of the genes involved in human pathologies are homologous to *Drosophila*, this organism can represent a useful model to identify mechanisms associated with different human diseases.[12,13] Despite the above mentioned, it is surprising that few studies have applied the *Drosophila* model to obtain new insights into the potential hazard resulting from MNPL exposure. Only four recent studies have been found in the literature. Two of them evaluated polystyrene (PS) MNPLs, and the other two used polyethylene (PET) MNPLs. Exposure to PSMNPLs resulted in gut damage, locomotor dysfunction, epigenetic silencing, and aggravated cadmium toxicity,[14] as well as somatic mutation and recombination in the wing imaginal disks.[15] On the other hand, exposure to PETMNPLs was associated with changes in fertility, the offspring of treated flies were smaller than the offspring of controls,[16] as well as decreased oviposition in exposed females and reduction of triglyceride and glucose content in male flies.[17]

In this context, the present study was planned to obtain information on a wide range of potential effects associated with exposure to PSMNPLs. Special attention has been dedicated, *via* transmission electron microscopy (TEM) images, to monitoring their journey into the intestine lumen, their potential interaction with different lumen components, their potential uptake by enterocytes, and their translocation through the intestinal barrier to the open circulatory system of the larvae, reaching hemocytes (as equivalent to lymphocytes in humans). In addition, the effects on the deregulation of different genes, as well as the induction of oxidative stress and genotoxicity, as detected by the induction of DNA breaks, were also systematically studied.

Materials and methods

Physicochemical properties of polystyrene nanoplastics

Nanopolystyrene particles, as a popular nanoplastic model, were purchased from Spherotech (Lake Forest, IL, USA). Most of the other chemicals and kits used in the different experiments were from Sigma Chemical Co. (St. Louis, MO, USA). To study the impact of size on the effects of plastic particles, three different sizes of polystyrene nanoplastics (PSNPLs) were selected: i) particles ranging from 50–100 nm (PS-50; SPH-PP-008-10), ii) particles ranging from 100–200 nm (PS-200; SPH-PP-015-10), and iii) particles ranging from 400–600 nm (PS-500; SPH-PP-05-10), according to the manufacturer's data. As the size range is in the nano range (1–1000 nm), they are all considered polystyrene nanoplastics (PSNPLs). They were supplied as a 0.02% sodium azide dispersion and stored at room temperature. To achieve the desired concentrations, PSNPLs were dispersed in Milli-Q-water. Particle suspensions were always vortexed before use. The characterization of the PSNPLs included several techniques and tools; a JEOL 1400 instrument (JEOL Ltd., Tokyo, Japan) for transmission electron microscopy (TEM) and a Malvern Zetasizer Nano-ZS zen3600 (Malvern, UK) instrument were used to detect the size, morphology, hydrodynamic size, and charge. In addition, Fourier-transform infrared spectroscopy (FTIR) using a Hyperion 2000 micro-spectrometer (Bruker, Billerica MA, USA) was used to confirm that all particles related to polystyrene share the same functional groups.

Toxic effects of polystyrene nanoplastics

The wild-type strain Canton-S was used in all the experiments. To evaluate the toxic effects of PS-50, PS-200, and PS-500 and to determine the appropriate doses to be used in the further experiments, *Drosophila* eggs were exposed to a wide range of concentrations: 0, 32, 160, and 800 μg mL^{-1}, which are equivalent to 0, 0.08, 0.4, and 2 mg PSNPLs per g food. Exposure lasts for all the developmental stages, until adult emergence. A total of 250 eggs per dose were seeded in five vials (50 eggs per vial) containing 4 grams of instant medium per vial. To hydrate the lyophilized instant culture medium, 10 mL of the different concentrations of PSNPLs were added to each vial. The emergent adults were

counted, and the viability percentage was calculated for each administered dose, in comparison with the unexposed flies.

Interaction of polystyrene nanoplastics with the intestinal barrier components

To investigate the interaction of PS-50, PS-200, and PS-500 with the different components of the larvae intestine, including enterocyte uptake, our previous protocol was followed.[18] Thus, about ten treated larvae (2 mg g^{-1} food), collected after the 5th day of exposure, were carefully washed and dissected in phosphate buffer solution to extract the intestinal tracts. After extraction, the intestines were directly immersed for 2 h in a fixation solution, post-fixed in 1% (w/v) osmium tetroxide containing 0.8% (w/v) potassium hexacyanoferrate, before washing four times with deionized water and sequential dehydration in acetone. Next, Eponate 12™ resin (Ted Pella Inc., Redding, CA) was used to embed the samples and left to polymerize at 60 °C for 48 h. Ultrathin sections (100 nm in thickness) were obtained by cutting the resin blocks with a diamond knife (45°, Diatome, Biel, Switzerland). Such ultrafine intestinal cuts were placed on non-coated 200 mesh copper grids and contrasted with uranyl acetate for 30 min and Reynolds lead citrate for 5 min. Finally, the sections were inspected using a JEOL 1400 (100 kV) TEM equipped with a CCD Gatan ES1000w Erlangshen camera (Gatan Inc, Pleasanton, CA). For these studies, evaluating the journey of PSNPLs inside the gut, only the higher dose was used just to facilitate their detection.

Detection of polystyrene nanoplastics in the hemolymph

To detect the potential translocation of PSNPLs through the intestinal barrier, their presence in the hemolymph was investigated. To proceed, samples of 5th day treated larvae were prepared and investigated according to our previous protocol.[19] Briefly, larvae were picked up with forceps, carefully cleaned, and dissected in buffer solution (PBS 1%) to obtain the hemolymph fluid. Hemolymph samples were collected and placed upon copper grids, left to dry, and investigated with a JEOL 1400 (100 kV) TEM to detect the presence of PSNPLs.

Detection of gene expression changes

Mild stress responses to PSNPL exposure can be detected *via* changes in the expression levels of specific genes In this study we proposed to investigate changes in the expression levels of general stress genes (heat-shock-protein-83, *Hsp83*, and heat-shock-protein-70, *Hsp70*), oxidative stress genes (Cu/Zn superoxide dismutase, Cu/Zn *Sod*; catalase, *Cat*, and superoxide dismutase-2, *Sod2*), DNA repair genes (8-oxoguanine DNA glycosylase, *Ogg1*), and two genes involved in the response to physical stress induced in the intestinal barrier (dual oxidase, *Duox*, and prophenoloxidase-2, *PPO2*). To this end, real-time RT-PCR was used to investigate gene expression levels as previously reported.[9] RNA was extracted following the manufacturer's protocol using 30 larvae (~50 mg) in the third-instar of development. The obtained RNA pellet was dissolved in Milli-Q water and quantitatively measured with a NanoDrop device. The RNA samples were used to synthesize cDNA using a transcriptor first strand cDNA synthesis Roche kit and were subjected to RT-PCR analysis using a Light Cycler 480 (Roche, Basel, Switzerland). The housekeeping gene β-actin was used as a reference gene. For all the genes, the same reaction conditions were applied: pre-incubation for 5 min at 95 °C, 1 cycle, and the amplification was repeated 45 times (10 s at 95 °C, 15 s at 61 °C, and 72 °C for 25 s).

Detection of oxidative stress induction

The levels of oxidative stress induced by the three selected sizes of PSNPLs were detected in the hemocytes of *Drosophila* larvae. To proceed, 5th day larvae treated with PS-50, PS-200, and PS-500 (0.0, 0.08, 0.4, and 2 mg g^{-1} food) were dissected in buffer solution (PBS 1%) to extract the hemolymph. The hemolymph was incubated with 5 μM 6-carboxy-2,7′-dichlorodihydro-fluorescein diacetate (DCFH-DA) for 30 min at room temperature to mark cells containing reactive oxygen species (ROS). For negative and positive controls, the hemolymph was extracted from non-treated larvae and larvae treated with 0.5 mM H_2O_2 for 30 min. Ten fluorescence images (fields) were taken using a fluorescence microscope, with an excitation wavelength of 485 nm and an emission wavelength of 530 nm (green filter). For the quantitative evaluation of fluorescent cells, both control and treated larvae from fluorescence images were quantified using the ImageJ program.

Detection of genotoxicity using the comet assay

The potential induction of DNA damage in hemocytes was investigated by using the comet assay, which can quantify the induction of DNA strand breaks. To proceed, third-instar (72 h) larvae treated with two doses (0.4 and 2 mg g^{-1} food) of PS-50, PS-200, and PS-500 were collected, washed, and kept in autoclaved phosphate buffer solution (PBS 1%). Unexposed larvae were used as a negative control, while larvae treated with 4 mM ethyl methanesulfonate (EMS) were used as a positive control. The used protocol has been previously described.[9] Ten μL of hemolymph, containing about 10 000 cells, was added to 90 μL of 0.75% low-melting agarose at 37 °C and mixed carefully. The mixture of cells and agarose was dropped upon the hydrophilic surface of a cold Gelbond® film (GBF). After lysis, electrophoresis, and neutralization steps, GBFs were stained with SYBERGold fluorochrome for 20 min and finally washed with distilled water. DNA break induction was measured according to the percentage of DNA in the tail using the Komet 5.5 image-analysis system (Kinetic Imaging Ltd., Liverpool, UK) fitted with an Olympus BX50 fluorescence microscope equipped with a 480–550 nm wide-band excitation filter and a 590 nm barrier filter. Three replicates of GBFs of 300 randomly selected cells per dose were used.

Statistical analysis

The normality and the homogeneity of the data were checked before performing the statistical analysis, using the Kolmogorov–Smirnov & Shapiro–Wilk test and Levene's test, respectively. For data with normal distribution and equal variance, Student's *t*-test and the one-way ANOVA were applied. The nonparametric analysis (Mann–Whitney U-test) was used for data with unequal variance or abnormal distribution. Significant differences were considered at $P \leq 0.05$. Data were calculated as mean ± standard error (SE).

Results

Physicochemical characteristics of PS-50, PS-200, and PS-500

To determine the effect of size, one PSNPL <100 nm (PS-50) and two PSNPLs >100 nm (PS-200 and PS-500) were characterized using different available tools like transmission electron microscopy (TEM), Malvern Zetasizer measurement, and FTIR spectroscopy to determine the size, morphology, degree of aggregation, hydrodynamic size, charge, and functional groups. The obtained results are shown in Fig. 1. The TEM images showed that all the studied PSNPLs agree with the range of sizes indicated by the supplier and show a spherical shape. The average diameter for PS-50, according to TEM, was 61.40 ± 14.72, for PS-200 the obtained average was 145.56 ± 9.0, and finally, for PS5-00 the average diameter was 415.22 ± 25.25. The spectra obtained from FTIR confirm that all chosen PSNPLs have the same functional groups of polystyrene. The peaks that appeared below 3000 cm^{-1} refer to CH_2, while those above 3000 cm^{-1} refer to the benzene ring, as confirmed by the strong peaks at 1500 cm^{-1}. These peaks are indicative of the functional groups that are identical to those of PS. Zetasizer data showed a trend similar to that obtained with TEM. The averages for the hydrodynamic sizes were 73.74 ± 1.88, 171.6 ± 3.94, and 488.9 ± 8.624 for PS-50, PS-200, and PS-500, respectively. All PSNPLs showed negative charges with zeta potential values of −49.7 ± 0.66, −49.6 ± 0.41, and −53.0 ± 1.99 for PS-50, PS-200, and PS-500, respectively. These zeta potential values indicate the good dispersion of the different PSNPLs.

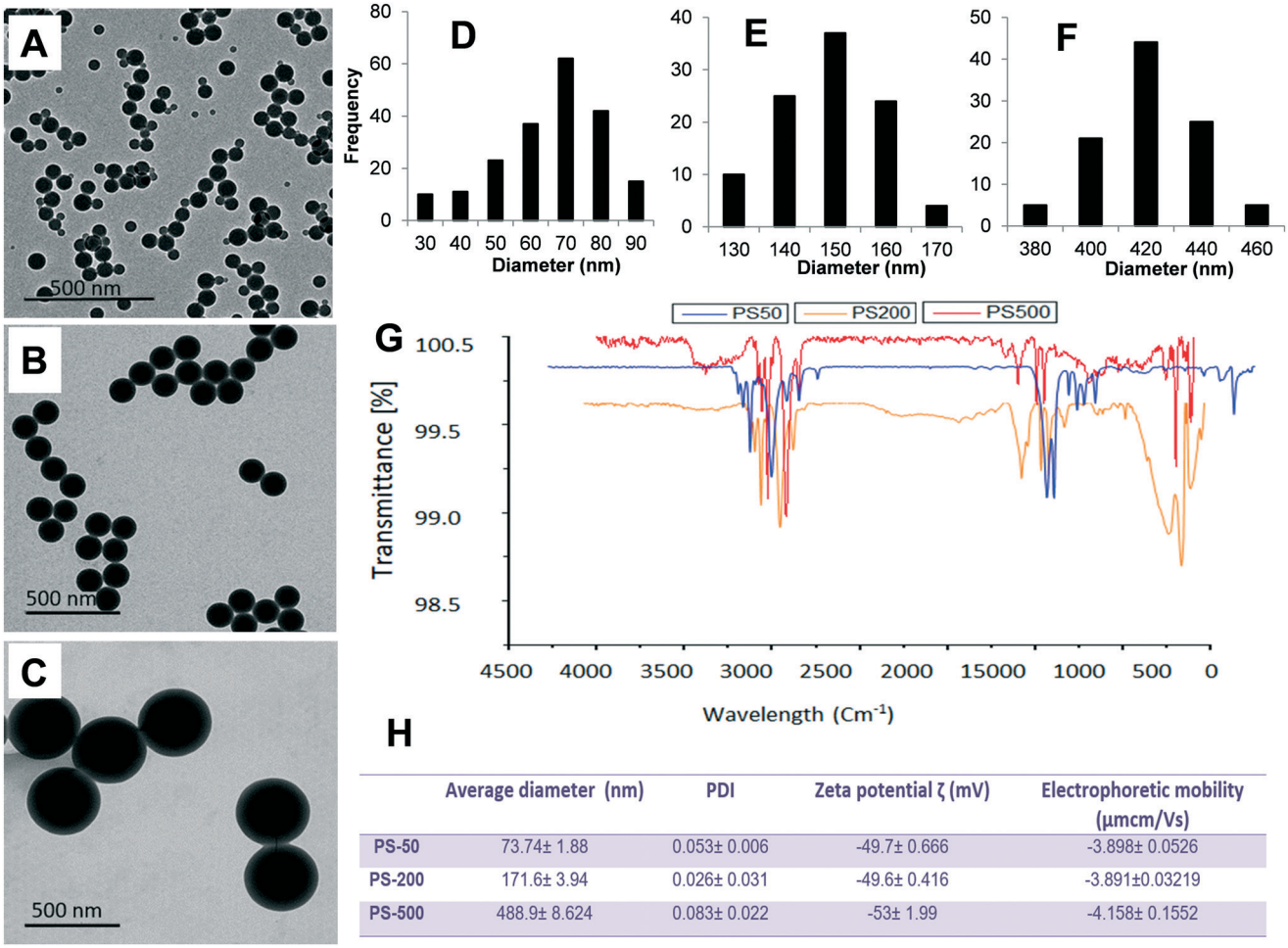

	Average diameter (nm)	PDI	Zeta potential ζ (mV)	Electrophoretic mobility (μmcm/Vs)
PS-50	73.74± 1.88	0.053± 0.006	-49.7± 0.666	-3.898± 0.0526
PS-200	171.6± 3.94	0.026± 0.031	-49.6± 0.416	-3.891±0.03219
PS-500	488.9± 8.624	0.083± 0.022	-53± 1.99	-4.158± 0.1552

Fig. 1 Physicochemical characteristics of different sized PSNPLs (PS-50, PS-200, and PS-500). The diameter averages of PS-50 (61.40 ± 14.72), PS-200 (145.56 ± 9.19), and PS-500 (415.22 ± 25.25) (D–F) were determined from different representative TEM images (A–C). To confirm the chemical composition of PSNPLs, Fourier transform infrared spectroscopy (FTIR) was applied to measure their functional groups (G). A Malvern Zetasizer instrument was used to determine the hydrodynamic size and zeta potential of the different PSNPLs (H).

Polystyrene nanoplastic toxicity

To detect the toxicity of the different sized PSNPLs, a defined number of eggs of *Drosophila* were seeded upon an instant medium, previously wetted with different concentrations of PSNPLs. The emergent adults were harvested and counted to calculate the percentage of adult survival after PSNPL exposure. The obtained results (ESI† Fig. S1) show that none of the different sized PSNPLs tested induced toxicity. No morphological changes or delays in the emergence of adults were observed associated with PSNPL exposure.

Monitoring of PSNPLs along the intestinal tract

The behavior of PSNPLs during their transit through the intestine can provide important information on their potential biological effects. To this end, we have described step by step all this long way starting from their entrance into the intestinal lumen, their interaction with different lumen components, their interaction with the intestinal barrier, their uptake and distribution inside enterocytes, and their potential translocation through the barrier reaching the hemolymph. All this information is shown in Fig. 2–4. The monitoring of the smallest particles (PS-50) is presented in Fig. 2(A–F). Thus, the particles are distributed in the midgut lumen (2A) and are observed to interact with the peritrophic membrane, which is the first line of the intestinal barrier defense. Interestingly PSNPLs are observed to be surrounded by extracellular membranes acting as carriers for their internalization (2B). PS-50 particles succeed to internalize into the enterocytes and are observed inside the cytoplasm especially surrounding the mitochondria (2C and 2D, respectively). PS-50 can translocate through the intestinal barrier as observed in the hemolymph of exposed larvae as individual particles (2E) or as aggregates (2F). The large size of polystyrene particles, whether PS-200 or PS-500, facilitated their detection during their internalization process. The internalization of PS-200 is presented in Fig. 3A–F. Thus, PS-200 particles are distributed inside the midgut lumen, surrounding symbiotic midgut bacteria, near the peritrophic membrane (3A). Interestingly, some PS-200 can penetrate the bacteria membrane to internalize inside the midgut bacteria (3B). PS-200 particles are also taken up by enterocytic cells facilitated by the presence of luminal vacuoles that appeared to engulf these particles to translocate them into enterocytes crossing the peritrophic membrane (3C and 3D). The particles just passing through the peritrophic membrane can be seen between the enterocyte microvilli and cytoplasm (3D and 3E). Finally, PS-200 can translocate towards the open circulatory system, as detected in the hemolymph (3F). The monitoring of PS-500 particles from ingestion to their translocation into the open circulatory system is presented in Fig. 4(A–D). After oral administration of PS-500 particles, their existence inside the midgut lumen can be detected easily due to their large size (4A). PS-500 can be detected near the peritrophic membrane to be ready to enter enterocytes (4B) or surrounding midgut bacteria (4C). The internalization into the enterocytes forming the intestinal barrier can be associated with the previous attachment to the peritrophic membrane or the engulfment by luminal vacuoles (4D). After their uptake by the intestinal barrier, PS-500 particles are distributed into the enterocyte cytoplasm (4E), being able to translocate towards the hemolymph (4F). As a summary, our results show that PSNPLs, independent of their size, can penetrate and cross the intestinal barrier reaching the open circulatory system as detected in the hemolymph.

PSNPL midgut erosion

Since the midgut lumen environment can affect the integrity of the administered PSNPLs, potential changes in their initial size were evaluated. The large size of the selected PSNPLs, especially PS-200 and PS-500, helps us to measure a sufficient

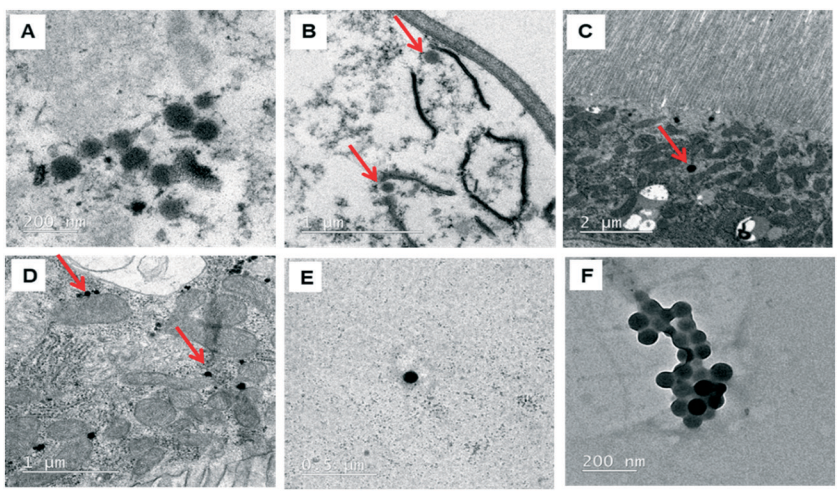

Fig. 2 Monitoring of ingested PS-50 from their ingestion until their translocation to the hemolymph compartment. PS-50 particles are distributed inside the midgut lumen (A), attached to the peritrophic membrane (B), inside the enterocyte cytoplasm (C), surrounding the mitochondria (D) and, finally, reaching the hemolymph (E and F).

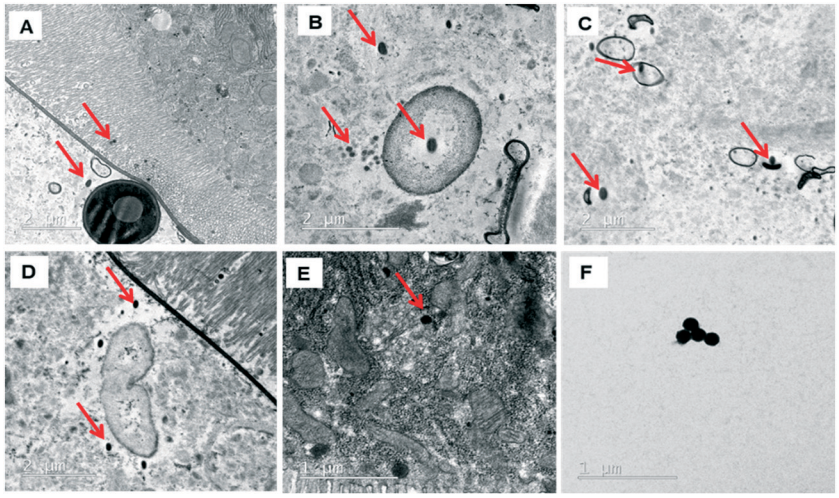

Fig. 3 Monitoring of PS-200 from their ingestion until their translocation to the hemolymph compartment. PS-200 particles are detected in the midgut lumen and enterocytes (A), surrounding/inside midgut bacteria (B), surrounded by/inside midgut vacuoles (C), near the peritrophic membrane or between microvilli (D), inside the enterocyte cytoplasm (E) and, finally, reaching the hemolymph (F).

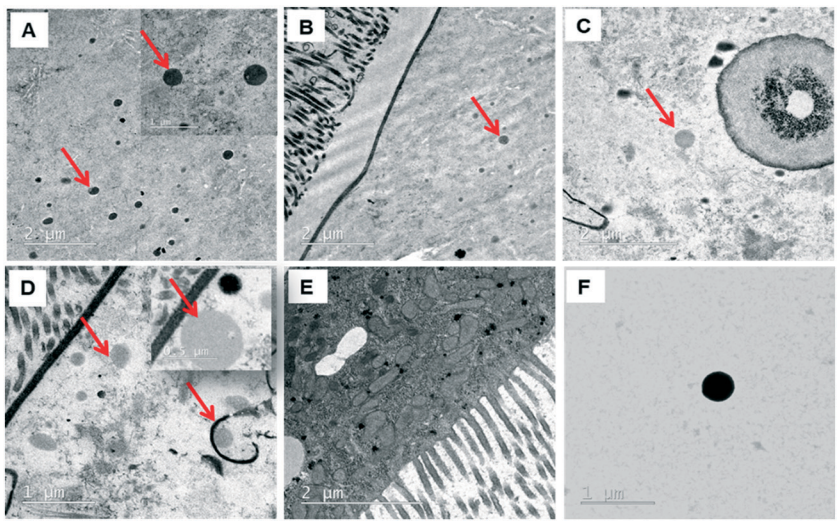

Fig. 4 Monitoring of PS-500 from their ingestion until their translocation to the hemolymph compartment. As occurs with the other sizes, PS-500 particles are detected inside the midgut lumen (A), surrounding the peritrophic membrane (B), surrounding midgut bacteria (C), inside the cytoplasm of enterocytes (D), surrounded by midgut vacuoles (E) and, finally, reaching the hemolymph (F).

number (70 particles per size) to determine their size both inside the midgut lumen and in previous oral administration (Fig. 5, A–F). The measured mean sizes inside the midgut lumen (141.90 ± 39.73 nm and 319.79 ± 97.45 nm) were compared with their initial sizes (145.56 ± 9.19 nm and 415.22 ± 25.25 nm) for PS-200 and PS-500 (5A and 5B, respectively). Measurements of the distribution of sizes for PS-200 and PS-500 inside the midgut lumen (5C and 5D) were done according to the representative TEM images (5E and 5F). In summary, our results have shown that PLNPLs with larger sizes are eroded inside the midgut lumen. This would indicate that when PSNPLs increase in size, they are more prone to erode during their intestinal transit, possibly due to chemical and mechanical stress.

PSNPL exposure modulates gene expression levels

The molecular response against any xenobiotic agents could give us an indication of their biological impact, acting as an early alarm of disturbance in the internal hemostasis balance. Accordingly, we checked the molecular response associated with PSNPL exposure in *Drosophila* larvae. A set of genes, previously evaluated in front of other nanomaterials,[20] were selected to determine the potential effects of PS-50, PS-200, and PS-500 (Fig. 6). The obtained results are indicated in the ESI.† The conserved stress genes, involved in the general stress response (*Hsp70* and *Hsp83*), are the first signal of molecular response, and their expression was significantly down-regulated with all the PSNPLs evaluated, regardless of

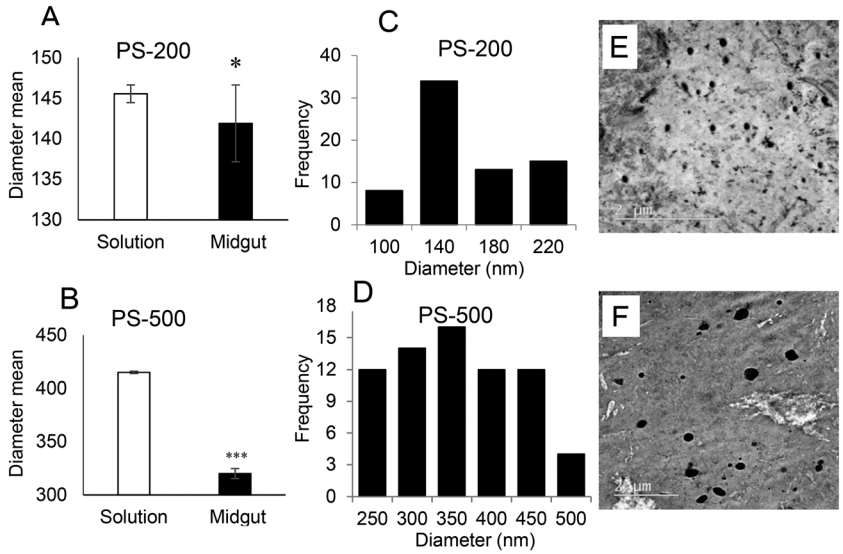

Fig. 5 PSNPL biodegradation inside the midgut lumen. Measurements of PS-200 and PS-500 diameters were carried out both in the administered dispersion and inside the midgut lumen, to check their ability to erode. The average diameter of PS-200 in solution (145.56 ± 9.19 nm) was a bit larger than that observed in the midgut lumen (141.90 ± 39.73 nm) (A). Regarding PS-500, the average in solution (415.22 ± 25.25 nm) was larger than that inside the midgut lumen (319.79 ± 97.45 nm) (B). The distribution of diameters for both P-200 and PS-500 is shown in C and D, respectively. These measurements were obtained from 70 PSNPLs of each size, whether in solution or in the midgut lumen. Representative TEM images are shown (E and F, respectively). Statistical significance $^{**}P < 0.01$, $^{***}P < 0.001$. Due to the lack of homogeneous variance and their abnormal distribution (especially for PS-200 data), the Mann–Whitney U-test was used for the statistical analysis.

their size; nevertheless, PS-50 produced more marked effects than PS-200 and PS-500. Regarding the antioxidant genes (*Cat*, *Sod2*, and Cu/Zn *Sod)*, the results showed that the exposure to PSNPLs, independent of their size, stimulated significantly the down-regulation of all the studied genes at all selected doses. The interaction of the internalized PSNPLs with the intestinal barrier, after oral administration, caused a down-regulation in the expression of *Duox* and *PPO2* in *Drosophila* larvae. Although the exposure to PS-200 and PS-500 induced a low effect upon the expression of *Duox*, PS-50 mediated a significant down-regulation for both genes *Duox* and *PPO2* at all tested doses. Finally, changes in the expression levels of the base excision repair (BER) gene *Ogg1* were determined showing that, regardless of their size, PSNPL exposure induced the down-regulation of *Ogg1* at all evaluated doses.

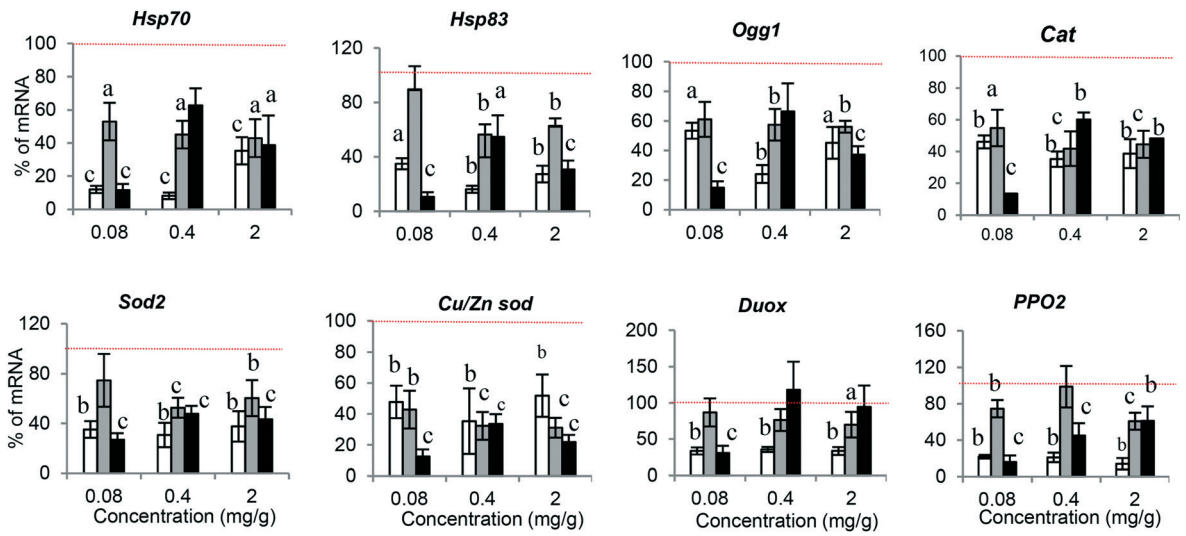

Fig. 6 Gene expression changes associated with polystyrene exposure. Different gene categories were investigated including stress genes: *Hsp70* and *Hsp83*; antioxidant genes: *Cat, Sod2*, and Cu/Zn *Sod*; DNA repair gene: *Ogg1* (F); and intestinal physical stress genes: *Duox and PPO*. Treated (120 h) and non-treated larvae were collected and stored at −80 °C. Changes in gene expression were detected using real time RT-PCR. The expression levels in PSNPL exposed larvae were compared with those in unexposed ones. Three different replicates per dose were used. (a) $P < 0.05$, (b) $P < 0.01$, and (c) $P < 0.001$. White color for PS-50, grey for PS-200, and black for PS-500.

Oxidative stress induction after PSNPL exposure

A key factor highlighting the negative impacts of exposure to PSNPLs is their ability to stimulate an oxidative stress status, *via* increasing the levels of reactive oxygen species (ROS). The results (Fig. 7A) indicate that PSNPLs, independent of their size, can elevate the ROS levels in hemocytes in a dose-dependent manner. This is especially observed for the smaller PSNPLs (PS-50 and PS-200) (Fig. 7C).

Genotoxicity of PSNPLs as evaluated with the comet assay

In the hazard assessment of any type of exposure, the induction of genotoxicity is of pivotal relevance. This is mainly related to the well-known association between DNA lesion induction and relevant consequences for human health. Among the different ways to detect the induction of DNA damage, the comet assay stands out, which detects the induction of DNA breaks. The obtained results show that the exposure to the different sized PSNPLs (PS-50, PS-200, and PS-500) induced significant increases in the levels of DNA damage, at all tested doses (Fig. 7B). Although all different PSNPLs mediated the genotoxic impact, the exposure to the smaller size (PS-50) induced higher levels of DNA damage (Fig. 7B).

Discussion

The term MNPLs hides two hot and unresolved topics, the frontiers between micro and nano ranges and the chemical nature of the plastics. Unfortunately, no agreement exists regarding these two points. If we accept the large experience gained in the field of engineered nanomaterials, where such materials are considered to range between 1 and 100 nm, by extension nanoplastics should cover the same range. Less agreement exists in the range covered by microplastics since many authors have considered that this size covers materials ranging from 1 μm to 5 mm, which assumes that the higher sizes escape from the micro-level. This complex scenario has been well presented by Hartmann *et al.*[21] who proposed to categorize MNPLs according to the conventional units of size: nano (1–1000 nm) and micro (1–1000 μm), although they realized that this proposal clashed with the accepted definition of nanoplastics (1–100 nm). To overcome this situation, they proposed to divide the nano range (1–1000 nm) between nanoplastics (1–100 nm) and submicron-plastics (100–1000 nm). Since the size is an important factor modulating the effects of nanomaterials,[22] we have selected in our study three different MNPL sizes: PS-50, PS-200, and PS-500. According to the above-mentioned classification, PS-50 belongs to the nanoplastic range, while PS-200 and PS-500

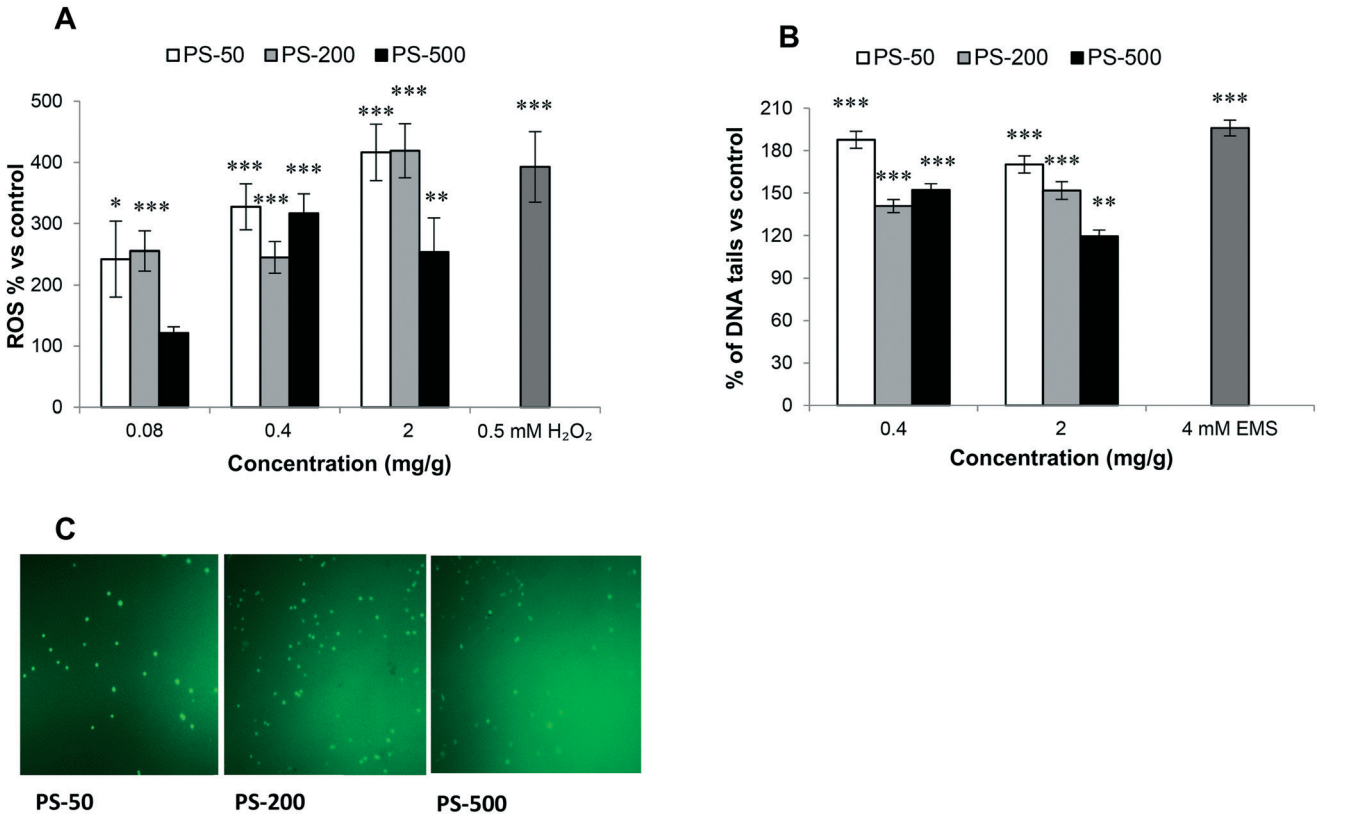

Fig. 7 The oxidative stress (A) and genotoxicity (B) induced in *Drosophila* larvae hemocytes after exposure (120 h) to different sizes (PS-50, PS-200, or PS-500) of PSNPLs in comparison with unexposed ones. Hydrogen peroxide and ethyl methanesulfonate (EMS) are used as positive controls. Representative fluorescence images for ROS detection. $*P < 0.05$, $**P < 0.01$ and $***P < 0.001$. White color for PS-50, grey for PS-200, and black for PS-500.

will match with the category of submicron-plastics. Nevertheless, to standardize the nomenclatures all of them are grouped as PS nanoplastics (PSNPLs). Regarding the chemical composition of the selected plastics, we have avoided the complexity of secondary microplastics by selecting pristine PSNPLs. The sizes, surface functionalization, and labeling of these commercial MNPLs have made them considered as standard MNPLs.

Our results showed that PSNPLs, regardless of their size, were unable to decrease adult emergence or reduce the viability of *Drosophila*, at all tested doses. This lack of toxic effects agrees with other two reported studies using *Drosophila* and different PSMNPL sizes.[14,15] This lack of toxicity is not entirely surprising because PSNPLs do not produce toxic effects when administered to different human cell cultures, including enterocytic Caco-2 cells.[23]

Since the main exposure route for MNPLs is ingestion,[24] there is a need for systematic studies to understand what occurs during their journey through the intestinal tract.[25] The *Drosophila* intestine is considered an emerging and versatile model system to study intestinal epithelial homeostasis and alterations induced by environmental agents.[26] In this context, we have gained experience in the monitoring of nanomaterials through the *Drosophila* intestinal transit which has been applied to the case of MNPLs.[20,27] The intestines of exposed larvae are obtained, and different transversal cuts are used to decipher the fate of the ingested MNPLs, by using TEM methodologies. This approach has permitted us to visualize the engulfment of MNPLs by luminal membranes, possibly originating from the peritrophic membrane, as a potential mechanism of uptake by the intestinal cells. It must be remembered that the peritrophic membrane in *Drosophila* is considered the first defense line, having a similar functional role to the mucus layer in the human intestine. More interesting is the observation of the interaction/uptake of MNPLs by the intestinal microbiota which could influence the functionality of that microbiome. Thus, their potential effects on gut microbiota dysbiosis are an attractive proposal in need of verification.[28] It should be indicated that *Drosophila* has been proposed as a simple model to study the microbiome,[29] and perturbations of its microbiome can result in states of instability or disease in *Drosophila*.[30]

The ingested PSNPLs can be subjected to interactions with midgut bacteria and with different intestinal enzymes, as well as with the acidic intestinal environment, potentially leading to decreases in their initial size; thereby, plastic particles can be eroded. These effects were confirmed in our study *via* measuring the diameters of PS particles in the midgut lumen and by comparing them with their diameters before oral administration. In this context, Yang *et al.*[31] found that the midgut' microorganisms plastic-eating mealworms can biodegrade polystyrene and form pits and cavities on its surface under enzyme activities secreted by the worm. In addition, in recent work, we have reported the tendency of intestinal digestive enzymes to induce biodegradation of ingested TiO_2 nanoparticles in *Drosophila* larvae.[29] In this context, it is important to note that we found some PSNPLs completely or partially surrounded with intestinal vacuoles and having rough shapes. Nevertheless, the knowledge on the biological effects of such morphological changes is far to be deciphered. The potential degradation ability of MNPLs by intestinal microbiota is a hot topic waiting for sound data. Although some results indicated that members of the phyla Actinobacteria and Firmicutes from *Lumbricus terrestris* were able to reduce the size of polyethylene MPLs,[32] there is a lack of rigorous studies to see if this does occur in humans or in other species.[33]

The advantage of our *in vivo* model of *the Drosophila* intestine is that we can visualize the uptake of PSNPLs by the intestinal cells, as well as their distribution inside the enterocytes constituting the intestine wall. This has not been reported, until now, in other well-used simple *in vivo* models like *Caenorhabditis elegans* and zebrafish.[34] According to our results, PSMNPLs distribute inside the cytoplasm of enterocytes and are observed surrounding the mitochondria. This looks like what was observed in Caco-2 cells, where this interaction induces morphological changes in the mitochondria[23] and mitochondrial dysfunction resulting from membrane disruption.[35]

Once internalized in the intestinal barrier, independent of the size, PSMNPLs succeed to translocate through the intestinal barrier completing their journey reaching the open circulatory system, where they are detected in the hemolymph. The presence of MNPLs in the hemolymph has been repeatedly observed in bivalves like *Mitillus*,[36] supporting their real ability to cross intestinal barriers. Once in the hemolymph, PSNPLs can reach the different tissues and organs. In this context, it is not rare to find that PSNPLs are incorporated into hemocytes, due to their phagocytic activity. Thus, our positive findings in *Drosophila* have also been observed in the hemocytes of the silkworm *Bombyx mori* larvae[37] and *Mitillus*.[36] Interestingly, several studies have reported the uptake of PSMNPLs by hemocytes of different organisms, but working *ex vivo*. In this case, they obtain the hemocytes of freshwater zebra mussels which are treated with different concentrations of PSMNPLs to demonstrate their phagocytic activity against MNPLs.[38] Interestingly this approach has also been applied to *Drosophila*.[39] In all the cases the phagocytosis of PSMNPLs by hemocytes was demonstrated. All these data confirm the ability of PSMNPLs to translocate through the intestinal barrier and their capacity to be incorporated, in a first instance, by hemocytes and possibly by cells from other organs/tissues. These results would agree with those obtained with PSNPLs in an *in vitro* model of the intestinal barrier, where a coculture of human intestinal cells Caco-2 (enterocytes) and HT-29 (goblet cells) was grown in an insert with a porous base. This insert was placed in a well with Raji-B cells (lymphocytes) simulating the blood compartment. Using fluorescent PSNPLs and confocal microscopy, the translocation *via* the intestinal barrier model and their uptake by Raji-B cells were demonstrated.[40]

At the molecular level, exposure to PSNPLs exhibits observable effects upon the expression of genes related to the maintenance of the intestinal barrier. The expression of *Duox* and *PPO2* genes was significantly deregulated after exposure to PSNPLs, regardless of their size, confirming their internalization *via* the intestinal barrier. Previously, we have reported the deregulation of this set of genes when *Drosophila* larvae were exposed to different nanomaterials.[20,27,41] Interestingly the induction of intestinal damage after exposure to PSMNPLs was also observed using trypan blue staining, which stained differentially the damaged and undamaged intestines of exposed and unexposed larvae.[14]

The distribution of PSNPLs in the intestinal and hemolymph compartments could produce toxic impacts at the level of cells, organs, or even on the whole organism. The toxic effects of ingested PSMNPLs have been mediated by ROS production in *Daphnia pulex*, especially by the smaller ones (100 nm), with a direct effect of the administered doses.[42] This type of mechanism has also been found to be involved in exposed *Daphnia*,[43] *C. elegans*,[44] and also in Wistar albino rats.[45] In agreement, we also found that despite size differences, ROS induction was directly associated with the exposure dose. The effects of PS-50 and PS-200 are more prominent than those caused by PS-500. Any change in the redox balance recalls the antioxidant machinery to store internal hemostasis.[46] In our case, the exposure to PSNPLs, independent of the size, significantly inhibited antioxidant gene expression (*Cat*, *Sod2*, and Cu/Zn *Sod*) at all tested doses, confirming the sensitivity of the antioxidant defense of *Drosophila* to PSNPLs. Similar results were obtained when *Daphnia pulex* was exposed to PSMNPLs, where the expression of *Cat*, *Sod2*, and Cu/Zn *Sod* was significantly decreased. This indicates the ability of PSMNPLs to induce overproduction of ROS coinciding with the inhibition of the antioxidant defense pathway.[42] Interestingly, the expression of Cu/Zn *Sod* was size-dependent, displaying the highest expression with the exposure to PS-50, and the lowest expression with the exposure to PS-500.

Regarding the expression of the general stress (*Hsp*) genes, they act as the first line of defense at the molecular level after environmental pollutant exposure. In our case, the exposure to the different sized PSNPLs inhibited the expression of *Hsp70* and *Hsp83*, at all tested doses. This downregulation agrees with that observed in goldfish where deregulation of *Hsp70* expression was observed after the exposure to two different PSMPLs, where such deregulations were size-dependent, like in our study.[47] This would indicate that PSMNPLs with small sizes mediate more prominent stress than those with higher sizes. In addition, the decrease in the expression of *Hsp* genes was associated with damaged intestinal epithelial cells in rats[48] or with the presence of potentially hazardous content inside the gut lumen, also in rats.[49]

It is assumed that oxidative stress resulting from MNPL exposure could initiate a genotoxic cascade of events. Nevertheless, and despite the relevance of the induction of DNA damage, the potential genotoxic risk of MNPL exposure presents many gaps and inconsistencies, mainly in *in vivo* models. Since it is well demonstrated that DNA damage is linked to drastic health consequences for humans,[50] obtaining sound genotoxicity data associated with MNPL exposures is of paramount relevance. In our study, we have evaluated the ability of PSNPLs to induce DNA breaks, which was evaluated in hemocytes using the comet assay. Significant increases in the levels of DNA damage after PSNPL exposure were observed. Although the effects were independent of the applied doses, an effect of size was detected, with an indirect relationship between the damage levels and the PSNPL size. These genotoxic effects of PSNPLs can be associated with the recently reported findings also in *Drosophila.* In that case, PSMPLs were used, and the genotoxic effects were detected using the wing spot assay that measures the induction of somatic mutation and recombination.[15] Interestingly, in a recent study on human lung epithelial A549 cells it has been reported that, despite the non-genotoxic potential of pristine plastics, the UV biodegraded particles produce DNA damage.[35] This could explain the genotoxic impact of PSNPLs in *Drosophila* larvae where they biodegraded and eroded the plastic material inside the gut lumen of the larvae. Noteworthily, the smaller PSNPS (PS-50 or PS-200 nm) produce more DNA damage, especially at the highest dose, than the PSNPLs with a larger size (PS-500). It should be noted that these findings correlate with their ability to cause oxidative stress. It is important to mention that the relationship of oxidative stress with genotoxicity and mutagenicity is well known.[51,52] Moreover, the exposure to PSNPLs caused down-regulation of the *Ogg1* gene expression, mainly at the highest dose. It must be remembered that the DNA glycosylase (*Ogg1*) enzyme constitutes the main defense line against the genotoxicity caused by oxidative DNA damage.[53] Taking all together, our results would confirm the genotoxic potential of PSNPLs in internal cells, once administered *via* ingestion. This would indicate that PSNPLs, mainly those with small size, can translocate *via* the intestinal barrier reaching the hemolymph with enough concentration to induce significant levels of DNA damage.

This study demonstrates the goodness of the *Drosophila* larvae intestinal model to monitor the journey of ingested MNPLs into the larval body. The sequence of pictures, showing their presence in the gut lumen and their interactions with different lumen components, gives us unequivocal visual information on such types of interactions. Furthermore, the model allows the detection of the translocation of MNPLs *via* the intestinal barrier by their presence in the hemolymph, as well as in the hemocytes. Their potential interaction with other cells from different tissues/organs remains to be solved. Although no relevant toxicity, as measured by the egg-to-adult viability, was observed independent of the PSNPL size, we obtained molecular pieces of evidence of general stress induction, as

well as of intestinal damage. Furthermore, significant induction of oxidative stress and DNA damage was observed in hemocytes. These effects were associated mainly with the PSNPL size, with higher effects induced by smaller sizes.

Author contributions

RM and AH planned the experiments. MA, DA, and JD carried out the experimental part. MA and DA analyzed the data, carried out the statistical analysis, and prepared the tables/figures. MA, DA, RM, and AH wrote the final manuscript.

Conflicts of interest

The authors declare that there is no conflict of interest.

Acknowledgements

This project has received funding from the European Union's Horizon 2020 research and innovation program under grant agreement No 965196. M. Alaraby was awarded a postdoctoral fellowship from the Cultural Affairs Sector and Missions (Ministry of Higher Education), Egypt.

References

1 S. Hohn, E. Acevedo-Trejos, J. F. Abrams, J. Fulgencio de Moura, R. Spranz and A. Merico, The long-term legacy of plastic mass production, *Sci. Total Environ.*, 2020, **746**, 141115.

2 S. B. Borrelle, J. Ringma, K. L. Law, C. C. Monnahan, L. Lebreton, A. McGivern, E. Murphy, J. Jambeck, G. H. Leonard, M. A. Hilleary, M. Eriksen, H. P. Possingham, H. De Frond, L. R. Gerber, B. Polidoro, A. Tahir, M. Bernard, N. Mallos, M. Barnes and C. M. Rochman, Predicted growth in plastic waste exceeds efforts to mitigate plastic pollution, *Science*, 2020, **369**, 1515–1518.

3 L. Rubio, I. Barguilla, J. Domenech, R. Marcos and A. Hernández, Biological effects, including oxidative stress and genotoxic damage, of polystyrene nanoparticles in different human hematopoietic cell lines, *J. Hazard. Mater.*, 2020, **398**, 122900.

4 T. Gouin, J. Avalos, I. Brunning, K. Brzuska, J. de Graaf, J. Kaumanns, Y. Koning, M. Meyberg, K. Rettinger, H. Schlatter, J. Thomas, R. van Welie and T. Wolf, Use of microplastic beads in cosmetic products in Europe and their estimated emissions to the North Sea environment, *SOFW J.*, 2015, **141**, 40–46.

5 C. Scherer, A. Weber, F. Stock, S. Vurusic, H. Egerci, C. Kochleus, N. Arendt, C. Foeldi, G. Dierkes, M. Wagner, N. Brennholt and G. Reifferscheid, Comparative assessment of microplastics in water and sediment of a large European river, *Sci. Total Environ.*, 2020, **738**, 139866.

6 L. Rubio, R. Marcos and A. Hernández, Potential adverse health effects of ingested micro- and nanoplastics on humans. Lessons learned from *in vivo* and *in vitro* mammalian systems, *J. Toxicol. Environ. Health, Part B*, 2020, **23**, 51–68.

7 Y. M. Cho and K. H. Choi, The current status of studies of human exposure assessment of microplastics and their health effects: a rapid systematic review, *Environ. Anal. Health Toxicol.*, 2021, **36**, e2021004.

8 C. Q. Y. Yong, S. Valiyaveetill and B. L. Tang, Toxicity of microplastics and nanoplastics in mammalian systems, *Int. J. Environ. Res. Public Health*, 2020, **17**(5), 1509.

9 M. Alaraby, B. Annangi, R. Marcos and A. Hernández, *Drosophila melanogaster* as a suitable *in vivo* model to determine potential side effects of nanomaterials: A review, *J. Toxicol. Environ. Health, Part B*, 2016, **19**, 65–104.

10 C. T. Ng, L. E. Yu, C. N. Ong, B. H. Bay and G. H. Baeg, The use of *Drosophila melanogaster* as a model organism to study immune-nanotoxicity, *Nanotoxicology*, 2019, **13**(4), 429–446.

11 M. C. Chifiriuc, A. C. Ratiu, M. Popa and A. A. Ecovoiu, Drosophotoxicology: an emerging research area for assessing nanoparticles interaction with living organisms, *Int. J. Mol. Sci.*, 2016, **17**(2), 36.

12 S. K. Kim, D. D. Tsao, G. S. B. Suh and I. Miguel-Aliaga, Discovering signaling mechanisms governing metabolism and metabolic diseases with *Drosophila*, *Cell Metab.*, 2021, **33**(7), 1279–1292.

13 M. Yamaguchi, I. S. Lee, S. Jantrapirom, K. Suda and H. Yoshida, *Drosophila* models to study causative genes for human rare intractable neurological diseases, *Exp. Cell Res.*, 2021, **403**(1), 112584.

14 Y. Zhang, M. B. Wolosker, Y. Zhao, H. Ren and B. Lemos, Exposure to microplastics cause gut damage, locomotor dysfunction, epigenetic silencing, and aggravate cadmium (Cd) toxicity in *Drosophila*, *Sci. Total Environ.*, 2020, **744**, 140979.

15 E. Demir, Adverse biological effects of ingested polystyrene microplastics using *Drosophila melanogaster* as a model *in vivo* organism, *J. Toxicol. Environ. Health, Part A*, 2021, **84**(16), 649–660.

16 E. Jimenez-Guri, K. E. Roberts, F. C. García, M. Tourmente, B. Longdon and B. J. Godley, Transgenerational effects on development following microplastic exposure in *Drosophila melanogaster*, *PeerJ*, 2021, **9**, e11369.

17 J. Shen, B. Liang, D. Zhang, Y. Li, H. Tang, L. Zhong and Y. Xu, Effects of PET microplastics on the physiology of *Drosophila*, *Chemosphere*, 2021, **283**, 131289.

18 M. Alaraby, A. Hernández, B. Annangi, E. Demir, J. Bach, L. Rubio, A. Creus and R. Marcos, Antioxidant and antigenotoxic properties of CeO_2NPs and cerium sulphate: Studies with *Drosophila melanogaster* as a promising *in vivo* model, *Nanotoxicology*, 2015, **9**, 749–759.

19 M. Alaraby, B. Annangi, A. Hernández, A. Creus and R. Marcos, A comprehensive study of the harmful effects of ZnO nanoparticles using *Drosophila melanogaster* as an *in vivo* model, *J. Hazard. Mater.*, 2015, **296**, 166–174.

20 M. Alaraby, A. Hernández and R. Marcos, Novel insights into biodegradation, interaction, internalization and impacts of high-aspect-ratio TiO2 nanomaterials: A systematic *in vivo* study using *Drosophila melanogaster*, *J. Hazard. Mater.*, 2021, **409**, 124474.

21 N. B. Hartmann, T. Hüffer, R. C. Thompson, M. Hassellöv, A. Verschoor, A. E. Daugaard, S. Rist, T. Karlsson, N. Brennholt, M. Cole, M. P. Herrling, M. C. Hess, N. P. Ivleva, A. L. Lusher and M. Wagner, Are we speaking the same language? Recommendations for a definition and categorization framework for plastic debris, *Environ. Sci. Technol.*, 2019, **53**(3), 1039–1047.

22 X. Wang, X. Cui, Y. Zhao and C. Chen, Nano-bio interactions: the implication of size-dependent biological effects of nanomaterials, *Sci. China: Life Sci.*, 2020, **63**(8), 1168–1182.

23 C. Cortés, J. Domenech, M. Salazar, S. Pastor, R. Marcos and A. Hernández, Nanoplastics as a potential environmental health factor: effects of polystyrene nanoparticles on human intestinal epithelial Caco-2 cells, *Environ. Sci.: Nano*, 2020, **7**(1), 272–285.

24 J. Domenech and R. Marcos, Pathways of human exposure to microplastics, and estimation of the total burden, *Curr. Opin. Food Sci.*, 2021, **39**, 144–151.

25 A. Poma, G. Vecchiotti, S. Colafarina, O. Zarivi, M. Aloisi, L. Arrizza, G. Chichiriccò and P. Di Carlo, *In vitro* genotoxicity of polystyrene nanoparticles on the human fibroblast Hs27 cell line, *Nanomaterials*, 2019, **9**(9), 1299.

26 F. Capo, A. Wilson and F. Di Cara, The intestine of *Drosophila melanogaster*: an emerging versatile model system to study intestinal epithelial homeostasis and host-microbial interactions in humans, *Microorganisms*, 2019, **7**(9), 336.

27 M. Alaraby, A. Hernández and R. Marcos, Systematic *in vivo* study of NiO nanowires and nanospheres: biodegradation, uptake and biological impacts, *Nanotoxicology*, 2018, **12**, 1027–1044.

28 J. Qiao, R. Chen, M. Wang, R. Bai, X. Cui, Y. Liu, C. Wu and C. Chen, Perturbation of gut microbiota plays an important role in micro/nanoplastics-induced gut barrier dysfunction, *Nanoscale*, 2021, **13**(19), 8806–8816.

29 A. E. Douglas, Simple animal models for microbiome research, *Nat. Rev. Microbiol.*, 2019, **17**(12), 764–775.

30 D. N. Lesperance and N. A. Broderick, Microbiomes as modulators of *Drosophila melanogaster* homeostasis and disease, *Curr. Opin. Food Sci.*, 2020, **39**, 84–90.

31 Y. Yang, J. Yang, W. M. Wu, J. Zhao, Y. Song, L. Gao, R. Yang and L. Jiang, Biodegradation and mineralization of polystyrene by plastic-eating mealworms: part 2. Role of gut microorganisms, *Environ. Sci. Technol.*, 2015, **49**(20), 12087–12093.

32 E. Huerta Lwanga, B. Thapa, X. Yang, H. Gertsen, T. Salánki, V. Geissen and P. Garbeva, Decay of low-density polyethylene by bacteria extracted from earthworm's guts: A potential for soil restoration, *Sci. Total Environ.*, 2018, **624**, 753–757.

33 E. Fournier, L. Etienne-Mesmin, C. Grootaert, L. Jelsbak, K. Syberg, S. Blanquet-Diot and M. Mercier-Bonin, Microplastics in the human digestive environment: A focus on the potential and challenges facing in vitro gut model development, *J. Hazard. Mater.*, 2021, **415**, 125632.

34 L. Lei, S. Wu, S. Lu, M. Liu, Y. Song, Z. Fu, H. Shi, K. M. Raley-Susman and D. He, Microplastic particles cause intestinal damage and other adverse effects in zebrafish *Danio rerio* and nematode *Caenorhabditis elegans*, *Sci. Total Environ.*, 2018, **619–620**, 1–8.

35 Q. Shi, J. Tang, X. Liu and R. Liu, Ultraviolet-induced photodegradation elevated the toxicity of polystyrene nanoplastics on human lung epithelial A549 cells, *Environ. Sci.: Nano*, 2021, **8**, 2660–2675.

36 M. Sendra, A. Saco, M. P. Yeste, A. Romero, B. Novoa and A. Figueras, Nanoplastics: from tissue accumulation to cell translocation into *Mytilus galloprovincialis* hemocytes. Resilience of immune cells exposed to nanoplastics and nanoplastics plus *Vibrio splendidus* combination, *J. Hazard. Mater.*, 2020, **388**, 121788.

37 C. C. Parenti, A. Binelli, S. Caccia, C. Della Torre, S. Magni, G. Pirovano and M. Casartelli, Ingestion and effects of polystyrene nanoparticles in the silkworm *Bombyx mori*, *Chemosphere*, 2020, **257**, 127203.

38 S. Magni, F. Gagné, C. André, C. Della Torre, J. Auclair, H. Hanana, C. C. Parenti, F. Bonasoro and A. Binelli, Evaluation of uptake and chronic toxicity of virgin polystyrene microbeads in freshwater zebra mussel *Dreissena polymorpha* (Mollusca: Bivalvia), *Sci. Total Environ.*, 2018, **631**, 778–788.

39 K. Adolfsson, L. Abariute, A. P. Dabkowska, M. Schneider, U. Häcker and C. N. Prinz, Direct comparison between *in vivo* and *in vitro* microsized particle phagocytosis assays in *Drosophila melanogaster*, *Toxicol. In Vitro*, 2018, **46**, 213–218.

40 J. Domenech, A. Hernández, L. Rubio, R. Marcos and C. Cortés, Interactions of polystyrene nanoplastics with *in vitro* models of the human intestinal barrier, *Arch. Toxicol.*, 2020, **94**(9), 2997–3012.

41 M. Alaraby, A. Hernández and R. Marcos, New insights in the acute toxic/genotoxic effects of CuO nanoparticles in the *in vivo Drosophila* model, *Nanotoxicology*, 2016, **10**(6), 749–760.

42 Z. Liu, Y. Huang, Y. Jiao, Q. Chen, D. Wu, P. Yu, Y. Li, M. Cai and Y. Zhao, Polystyrene nanoplastic induces ROS production and affects the MAPK-HIF-1/NFkB-mediated antioxidant system in *Daphnia pulex*, *Aquat. Toxicol.*, 2020, **220**, 105420.

43 W. Lin, R. Jiang, S. Hu, X. Xiao, J. Wu, S. Wei, Y. Xiong and G. Ouyang, Investigating the toxicities of different functionalized polystyrene nanoplastics on *Daphnia magna*, *Ecotoxicol. Environ. Saf.*, 2019, **80**, 509–516.

44 H. Chen, X. Hua, H. Li, C. Wang, Y. Dang, P. Ding and Y. Yu, Transgenerational neurotoxicity of polystyrene microplastics induced by oxidative stress in *Caenorhabditis elegans*, *Chemosphere*, 2021, **272**, 129642.

45 A. A. Babaei, M. Rafiee, F. Khodagholi, E. Ahmadpour and F. Amereh, Nanoplastics-induced oxidative stress, antioxidant defense, and physiological response in exposed Wistar albino rats, *Environ. Sci. Pollut. Res.*, 2022, **29**, 11332–11344.

46 H. Sies, Oxidative stress: a concept in redox biology and medicine, *Redox Biol.*, 2015, **4**, 180–183.

47 S. Abarghouei, A. Hedayati, M. Raeisi, B. S. Hadavand, H. Rezaei and A. Abed-Elmdoust, Size-dependent effects of

microplastic on uptake, immune system, related gene expression and histopathology of goldfish (*Carassius auratus*), *Chemosphere*, 2021, **276**, 129977.

48 P. C. Yang, Y. H. Tu, M. H. Perdue, C. Oluwole and S. Struiksma, Regulatory effect of heat shock protein 70 in stress-induced rat intestinal epithelial barrier dysfunction, *N. Am. J. Med. Sci.*, 2009, **1**(1), 9–15.

49 J. H. Ovelgönne, J. F. Koninkx, A. Pusztai, S. Bardocz, W. Kok, S. W. Ewen, H. G. Hendriks and J. E. van Dijk, Decreased levels of heat shock proteins in gut epithelial cells after exposure to plant lectins, *Gut*, 2000, **46**(5), 680–688.

50 M. Carbone, S. T. Arron, B. Beutler, A. Bononi, W. Cavenee, J. E. Cleaver, C. M. Croce, A. D'Andrea, W. D. Foulkes and G. Gaudino, *et al.*, Tumour predisposition and cancer syndromes as models to study gene-environment interactions, *Nat. Rev. Cancer*, 2020, **20**, 533–549.

51 A. Barzilai and K. I. Yamamoto, DNA damage responses to oxidative stress, *DNA Repair*, 2004, **3**(8–9), 1109–1115.

52 Y. Baiken, D. Kanayeva, S. Taipakova, R. Groisman, A. A. Ishchenko, D. Begimbetova, B. Matkarimov and M. Saparbaev, Role of base excision repair pathway in the processing of complex DNA damage generated by oxidative stress and anticancer drugs, *Front. Cell Dev. Biol.*, 2021, **8**, 617884.

53 A. Bravard, M. Vacher, B. Gouget, A. Coutant, F. H. de Boisferon, S. Marsin, S. Chevillard and J. P. Radicella, Redox regulation of human OGG1 activity in response to cellular oxidative stress, *Mol. Cell. Biol.*, 2006, **26**(20), 7430–7436.